



# Ultrasound Waves Effect on the Proliferation of Fibroblast Cells: Collagen Type I Expression

Zeinab Hormozi Moghaddam (PhD)<sup>1</sup>, Manijhe Mokhtari-Dizaji (PhD)<sup>1\*</sup>, Mohammad Ali Nilforoshzadeh (MD, PhD)<sup>2</sup>, Mohsen Bakhshandeh (PhD)<sup>3</sup>

## ABSTRACT

**Background:** Ultrasound waves are considered non-invasive, safe, and mechanical stimuli with unknown mechanisms.

**Objective:** The aim of this study is to determine the effect of acoustic cavitation interaction according to the mechanical index (MI) on fibroblast cells' reproducibility and gene expression of collagen I as a skin repair agent.

**Material and Methods:** In this interventional study, the ultrasonic pressure equations were solved to extract the maximum mechanical indices with frequencies of 150 kHz, 40 kHz, 28 kHz and low intensity ( $<0.5 \text{ W/cm}^2$ ). Groups were extracted with a mechanical index of 0.10, 0.20, and 0.40. Then, fibroblast cells were exposed to selected acoustic parameters from simulation. After 5 days, the proliferation was measured with an MTT (3-(4, 5-Dimethylthiazol-2-yl)-2, 5-diphenyltetrazolium bromide) assay, and collagen I expression was quantified.

**Results:** Increasing reproducibility in the groups of  $0.23 \text{ W/cm}^2$  with 0.20 mechanical index threshold was calculated at  $1.70 \pm 0.05$  and  $1.07 \pm 0.04$  times higher in continuous and pulse modes compared to the control group. Reducing the proliferation in group 0.40 mechanical index was shown as compared with control and sham groups in pulse mode ( $P\text{-value} < 0.05$ ). The collagen I expression level of fibroblast cells in groups of control and 0.20 MI were  $0.03 \pm 0.00$  and  $0.17 \pm 0.05$ , respectively. The acoustic vibration effects at 0.20 mechanical index have promoted fibroblast cell functions.

**Conclusion:** Low-frequency and -intensity ultrasound waves on the mechanical index threshold (cavitation threshold) increases the proliferation of fibroblast cell and the expression of collagen type I.

**Citation:** Hormozi Moghaddam Z, Mokhtari-Dizaji M, Nilforoshzadeh MA, Bakhshandeh M. Ultrasound Waves Effect on the Proliferation of Fibroblast Cells: Collagen Type I Expression. *J Biomed Phys Eng*. 2025;15(3):249-262. doi: 10.31661/jbpe.v0i0.2212-1567.

## Keyword

Ultrasound Waves; Proliferation; Collagen Type I; Cavitation; Mechanical Index

## Introduction

In recent years, ultrasound is increasingly considered a bioactive therapeutic tool because of its wide scope of natural, biological, and biochemical effects in vitro [1, 2]. Low-intensity Ultrasound (LIUS) as a type of physical stimulation factor can promote tissue regeneration by improving blood circulation, accelerating wound healing, and stimulating angiogenesis [3]. The fundamental processes can enhance growth factors or signaling molecules, facilitate differentiation, and produce extracellular matrix in cell and tissue repair [4]. A fibroblast is a

<sup>1</sup>Department of Medical Physics, Faculty of Medical Sciences, Tarbiat Modares University, Tehran, Iran

<sup>2</sup>Skin and Stem Cells Research Center, Tehran University of Medical Sciences, Tehran, Iran

<sup>3</sup>Department of Radiology Technology, Allied Medical Faculty, Shahid Beheshti University of Medical Sciences, Tehran, Iran

\*Corresponding author: Manijhe Mokhtari-Dizaji  
Department of Medical Physics, Faculty of Medical Sciences, Tarbiat Modares University, Tehran, Iran  
E-mail: mokhtarm@modares.ac.ir

Received: 1 December 2022  
Accepted: 24 April 2023

significant form of cell in the connective tissue that synthesizes the Extracellular Matrix (ECM) and collagen and is also essential for the reconstruction and remodeling of tissue after injury [5]. In this regard, collagen type I is the most common type of collagen and plays a functional key role in skin tissue [6]. Collagen types I and II have significant roles in the regeneration of tissue by fibroblast cells [7, 8]. The process of fibroblast proliferation, secretion of growth factors, and synthesis of collagen seem essential to treat wound healing. One method for realizing the process of stimulation on fibroblast function and collagen gene expression is the isolation, culture, reservation, and proliferation of fibroblast cells in vitro [9, 10].

In addition, the healing of skin injuries requires complicated interactions of the ECM, dermal, and epidermal cells. Mechanical and chemical stimuli activated the intracellular signaling pathways [11, 12]. Therefore, it is important to select the optimal parameters for stimulation of the signal pathways to repair the damage and increase cell proliferation. Mechanical stimulations are among the essential factors for the proliferation of cell and stem cells and the stimulation of special intracellular signal pathways [13].

LIUS is now widely used for several purposes. Suspension-cultured hazel cells were sonicated with LIUS. Treatment stimulated the production of major taxanes. Increased release of taxanes by ultrasound resulted likely from stimulation of taxane biosynthesis [14]. LIUS may increase the fibroblast growth factor and expression of collagen type I through its advantages such as non-invasiveness and ease to use. The previous study was shown that low-intensity ultrasound with low frequency did not alter temperature, and the positive effects of LIUS could be caused by non-thermal effects [15]. Such mechanical stimulation triggers a specific signaling platform [16].

Cellular responses to LIUS are parameter-dependent with specific exposure conditions.

Ultrasound biological effects are thermal and non-thermal (vibration or ultrasound-induced cavitation). Despite various advances, the actual mechanisms of interaction between ultrasound and acoustic cavitation with cells and its effectiveness have not been clear yet in proliferation and gene expression in tissue repair [13, 15-17].

Studies indicated that low-frequency ultrasound has more effective therapeutic impacts than high-frequency ultrasound [15-17]. Hence, frequencies below 200 kHz are especially noticed and studied in the field of tissue regeneration and cell activity. Acoustic cavitation is a term that describes the effect of ultrasound on the formation, growth, oscillation, and collapse of cavities in a liquid medium. If the negative acoustic pressure is high enough, bubbles form in the half cycle of expansion. To understand the biological effects of acoustic cavitation of ultrasound with a low-intensity ( $<2 \text{ W/cm}^2$ ) and low-frequency ( $<200 \text{ kHz}$ ), it is necessary to analyze the effect of interactions between acoustic waves and biological medium [16]. Moreover, in vitro studies using cell culture can lead to understanding the phenomena of the proliferation of fibroblast and collagen synthesis, including the main histological changes observed in wounds treated with bio-stimulation; these effects require specific exposure conditions. For example, a 0.20 Mechanical Index (MI) is a threshold of induced acoustic cavitation in water or culture medium [16]. In the present study, the effect of the mechanical index of low-frequency sonication was evaluated on the proliferation and collagen I expression of fibroblast cells.

## Material and Methods

In this interventional study, MI was introduced to investigate the effects and safety levels of low-frequency ultrasound waves in therapeutic and cellular applications. The mechanical index is applied to define the threshold of cavitation. In the present study, acoustic cavitation interaction is investigated using

acoustic pressure and MI modeling of low-frequencies to optimize the mechanical transmission pathways in fibroblast cells. The radiation parameters are then extracted, including the frequency, intensity, and distance of the culture plate, and fibroblast cells irradiated at pulse and continuous modes.

According to Rayleigh's equation, low-intensity and, low-frequency ultrasound parameters are obtained by acoustic pressure and MI modeling [17, 18]. The Mechanical index higher and lower than the threshold of 0.20 were selected to examine the mechanical interaction, such as the micro-streaming, the acoustic cavitation, and collapse interaction, in vitro [16]. The analytical solution of acoustic pressure,  $P(r')$ , and the MI are obtained through an acoustic propagation equation. The conditions for solving the equation are given as follows [17, 18]:

$$P(r') = ikcp_t \iint \frac{u}{2\pi r'} \exp^{-(\alpha+ik)r'} dS \quad (1)$$

$$u = u_0 e^{i\omega t} \quad (2)$$

where  $u$  and  $u_0$  denote the amplitude of the oscillation speed of the crystal surface and the amplitude or initial oscillation speed. Also,  $k$ ,  $\rho t$ ,  $c$ ,  $\alpha$ ,  $ds$ ,  $\omega$ , and  $r$  are wave number, the density of the tissue, speed of acoustic propagation in the medium, absorption coefficient, elements of the transducer, angular frequency, and distance of crystal surface to the target, respectively. Considering the disc shape of the crystal, cylindrical coordinates are selected to solve the equation. According to Equation 3, Rayleigh integral pressure equation considers an acoustic transducer infinite element with a suitable size and less than the sound wavelength, acting as a point acoustic source [18]:

$$P(r, \theta, z, t) = \frac{ikP_s}{2\pi} \exp(i\omega t) \iint \frac{\exp(-(a+ik)r)}{r} \quad (3)$$

The ultrasound interaction of these sources involves constructive and destructive interference. Finally, the acoustic pressure is measured through the sum of the waves and

calculating the pressure for each point [19]. The acoustic pressure equation in cylindrical coordinates with transducer cross-section and culture plate cross-section to the desired distance was solved in FORTRAN (Microsoft Fortran Power Station 4.0, MathWorks Co., MA, USA) language and a computer with a processor (Core™ i5-4200M CPU- 2.50 GHz- 6 GB RAM, Australian Co., Sydney, Australia). Calculations were done using the following parameters: water temperature of water 37 °C, a density of 1000 kg/m<sup>3</sup>, a sound propagation speed of 1528 m/s, and an attenuation coefficient of 0.002 N/MHz. Figure 1 (a-b) depicts the effects of ultrasound waves on cells based on radiation geometry and experimental setup. The experimental setup includes a transducer, impedance-matching gel, cell culture plate, and ultrasound absorber to prevent the formation of standing waves.

A low-frequency transducer with 150 kHz, 40 kHz, and 28 kHz and low-intensity (<0.5 W/cm<sup>2</sup>) in continuous exposure mode and the radius of the target (1.8 cm) were considered an input variable to extract the MI.

Based on the physical input parameters, the ultrasonic pressure was calculated and the minimum acoustic pressure was obtained at intervals with 10<sup>-5</sup> m spatial resolution at each point. In specified  $z$ ,  $r$ , and  $\theta$ , MI was determined by solving the pressure equation at each point similar to Figure 1b [16]:

$$[MI = \frac{P_{min}}{\sqrt{f}}] \quad (4)$$

$P_{min}$  and  $f$  are the minimum acoustic pressure and frequency, respectively. Figure 1c presents a contour of ultrasonic pressure in cylindrical coordinates with culture plate cross-section ( $r=1.87$  cm).

Experiments were done in the Faculty of Medical Sciences, Tarbiat Modares University, Tehran, Iran. All of the studies followed the guidelines of the Laboratory Animal Ethical Commission. Fibroblast cells of guinea pig skin tissue were selected because these cells have a high resemblance to the human

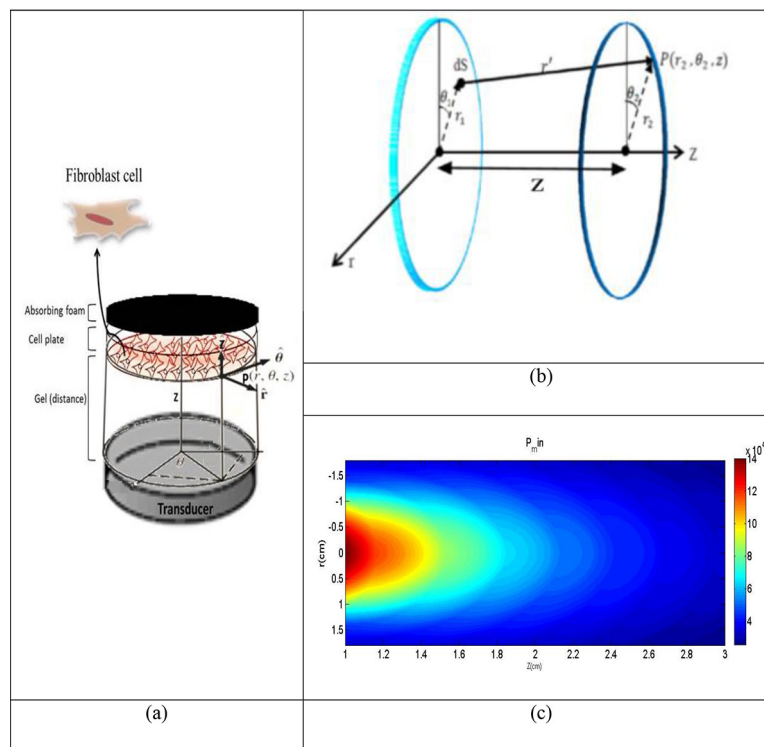


**Figure 1:** The acoustic pressure model of low-frequency ultrasound: **a)** the setup of the transducer and cell culture plate, absorbing foam prevents the creation of standing waves, **b)** geometry in the modeling in cylindrical coordinates, and **c)** the axial contour  $[r \text{ (cm)}]$  of acoustic pressure  $[P_m]$ .

skin model. Hartley Dunkin Guinea pigs ( $n=5$ ) with a mean weight of 450-500 g were used in the experiments and euthanized by an intraperitoneal injection of ketamine 10% and xylazine 2% (Alfasan, Woerden, Holland). The skin of the neck or abdomen was immediately removed and washed in sterile Phosphate-buffered Saline (PBS; Gibco, UK) containing 1% penicillin and streptomycin. The skin was cut into small pieces ( $1 \text{ mm}^2$ ) and explanted in Dulbecco's Modified Eagle Medium (DMEM; Gibco cat. number 12800-116), 10% Fetal Bovine Serum (FBS; Gibco, UK), 1% penicillin and streptomycin, and 1% L-glutamine in 6 well culture plate and were cultured at  $37^\circ\text{C}$  in an incubator with 5%  $\text{CO}_2$  and saturated humidity. The medium was replaced after 48 h. During the expansion, the medium was replaced every 2-3 days. Fibroblast cells were grown on the skin explant, after ten days.

When fibroblast cells reached 80-90% confluence, the cells were harvested using 0.25% trypsin (Gibco, UK) and transferred to the next passage. Images were captured with an Olympus microscope (ix70 model, Olympus Co, Tokyo, Japan).

A total of  $10^4$  fibroblast cells were placed at different distances according to various MI to evaluate the effect of ultrasound waves on proliferation. The groups consisted of three treatments referred to as 0.10, 0.20, and 0.40 MI groups, compared with control and sham groups at continuous mode and pulse mode. Cells cultured in an enclosed sterile 3.5 cm tissue culture plate in an incubator ( $37^\circ\text{C}$ ) were sonicated. The transducer was placed at the bottom of the cell plate, and ultrasound waves were transmitted through coupling gel into the cell plate. The effect of the ultrasound waves was investigated on fibroblast cells at



continuous mode and 20% pulse mode with a Pulse Repetition Frequency (PRF) of 0.5 Hz. The acoustic cavitation rate in PRF of 0.5 Hz was significantly higher than that of other PRF (3, 5, and 10 Hz) [20].

The culture medium at 37 °C with the intensity and frequency corresponding to the selected MI was radiated under ultrasound waves. The medium temperature was measured by a digital thermometer (Multilogger Thermometer CHY/502A, Taiwan,  $\pm 1$  °C). There was a micro-thermocouple channel in the culture medium and another one on the outside. After recording the results, the sonication time was determined lower than the hyperthermia level. This study was conducted to reduce the thermal effects of ultrasound waves. Thermal monitoring was repeated three times on a 3-day duration.

Fibroblast cells were incubated into a sterile 3.5 cm culture plate with 104 density of cells in passages 3-4 and maintained in DMEM with FBS (10%). Then, they were exposed with 0.10, 0.20, and 0.40 MIs as treatment groups in an incubator (37 °C), after 24 h. After sonication, cells were incubated for five days. The control and the sham groups were cultured in 10% FBS in the DMEM medium without sonication. The ratio of optical density (OD) of cells in MTT (3-(4, 5-Dimethylthiazol-2-yl)-2, 5-diphenyltetrazolium bromide) assay was extracted. Briefly, 10  $\mu$ l MTT was added to 100  $\mu$ l of DMEM on each plate. After 6 h of incubation, 100  $\mu$ l of Dimethyl Sulfoxide (DMSO) was added to 100  $\mu$ l of DMEM in each plate and the optical density (OD) was determined by a microplate reader (Multi-Mode Microplate Readers, BioTek,  $\lambda=570$  nm). The MTT standard curve was plotted to estimate the cell number (1,000-80,000 cells) based on optical density [21].

The focus of the present study is on the collagen transcriptional level in the fibroblast cells of the guinea pig. In response to external mechanical stimuli on fibroblast cells, collagen I is the most abundant collagen synthesized

from fibroblast cells in tissue repair. Hence, total Ribonucleic Acid (RNA) was harvested on a 5-day similarity MTT assay after 3-day ultrasound exposure in vitro to evaluate the effect of the MI with the most effect on reproducibility [22]. RNA of fibroblast cells was achieved by RiboEx total RNA (RNX). According to the manufacturer's protocol, total RNA was reversed and transcribed to cDNA by Prime Script RT reagent Kit with a cDNA eraser [23].

Reverse Transcription Polymerase Chain reaction (PCR) oligonucleotide primers were used as primers: collagen type 1 (F: 5'-GGCTGCACGAGTCACACA-3' and R: 5'-TGGAGGGAGTTTACACGAAGC-3') and the internal control  $\beta$ -actin (F: 5'-AGACGAAGCCCAGAGCAAAAG-3' and R: 5'-GCCAGAGGCATACAGGGACAG-3'). Using the Oligo 7 software, the Primer was designed based on the homology method. The PCR oligonucleotide primers have been published at the National Center for Biotechnology Information (NCBI), with locus LC386214. Realtime PCR using Fluorescent Dyes SYBR Green: BioFACTTM2X qPCR Master Mix was used for quantification of gene expression. Reactions have taken place in the StepOne™ v2.3 software. Reactions were performed on the StepOne™ v2.3 software. The expression of  $\beta$  Action was used for the standardization of real-time PCR results. For each reaction, a melting curve was generated to rule out primer formation of dimer and false priming, followed by calculating the  $2^{-\Delta Ct}$  (fold change) and  $2^{-\Delta Ct}$  (expression level) to determine relative levels of mRNA. Next, the cDNA of each sample was examined using agarose electrophoresis [23].

The results of 10 groups with 0.10, 0.20, and 0.40 MI, sham, and control after continuous and pulsed LIUS (20%) presented as mean  $\pm$  standard deviation (SD), and one-way ANOVA test were used to analyze differences between groups, at a significant level of 0.05 ( $P$ -value < 0.05). Also, the dependence

between the cell proliferation and collagen I expression level at continuous and pulse modes was studied by Pearson correlation analysis. All treatments were done with three independent replicates. All data were analyzed using the SPSS statistical v20 software (SPSS/PC Inc., Chicago, IL).

## Results

The changes in acoustic pressure at different points from the surface of the transducer were calculated. Figure 2 presents the plot of transducers of 150, 40, and 28 kHz at different intensities on a target with a radius of 1.8 cm.

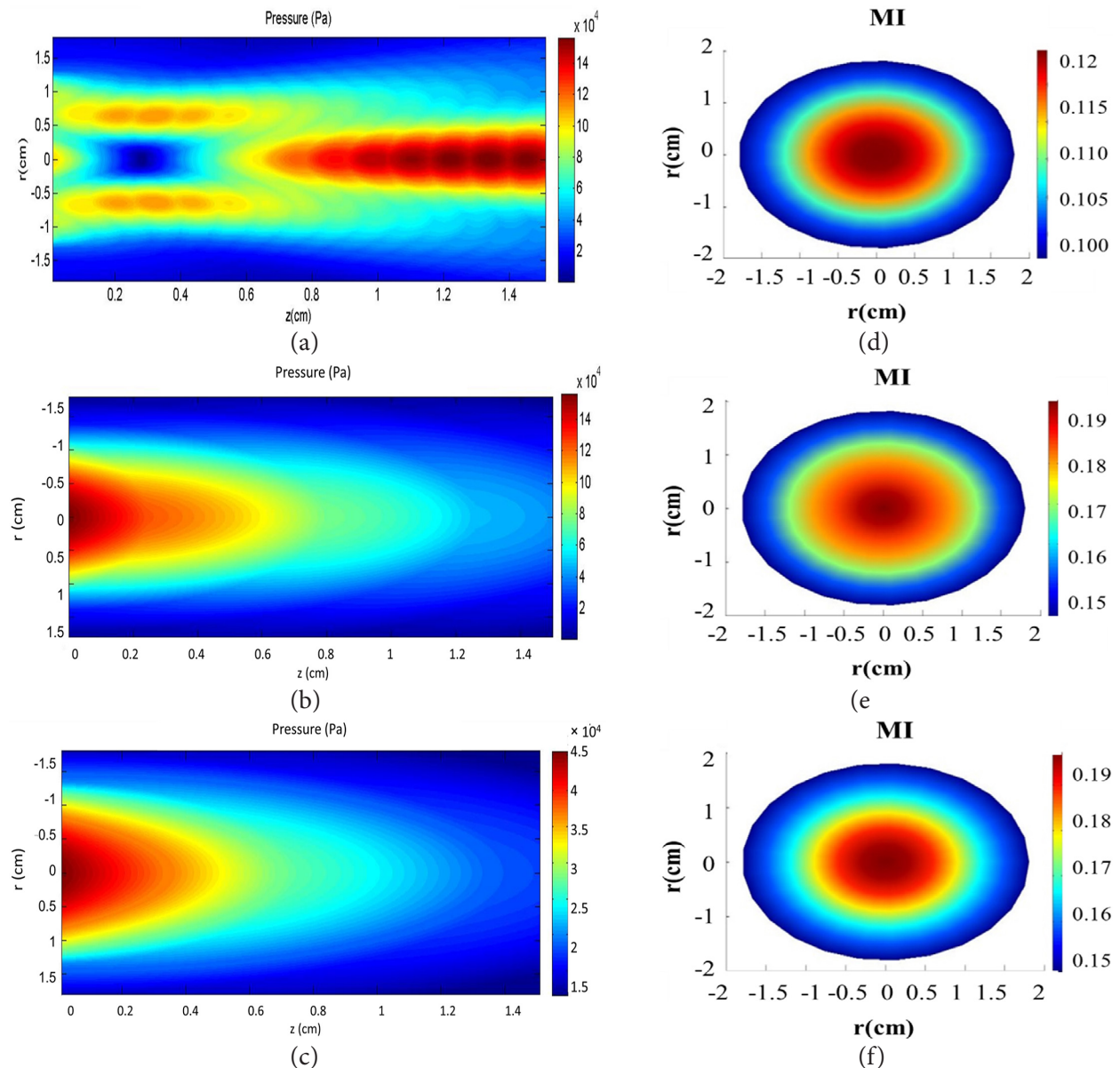


**Figure 2:** The axial contour of acoustic pressure on the r-z screen: **a)** 150 kHz, (Mechanical Index) MI=0.35, **b)** 40 kHz, MI=0.50, and **c)** 28 kHz, MI=0.20 in near-field depth. The horizontal axis shows the z-axis (cm) and the vertical axis shows minimal acoustic pressure (MPa). Color changing from blue to red suggests an increase in acoustic pressure up to  $14 \times 10^4$  Pa at 150 kHz and 40 kHz and up to  $4.5 \times 10^4$  Pa at 28 kHz. The radius profile of a MI is shown for 40 kHz frequency, in which the color map shows the MI range: **d)** 0.10 MI, 0.12 W/cm<sup>2</sup>, 3 cm, **e)** 0.20 MI, 0.23 W/cm<sup>2</sup>, 2.5 cm, and **f)** 0.40 MI, 0.30 W/cm<sup>2</sup>, 1 cm. Vertical and horizontal axes are in cm.

According to contours in Figure 2, ultrasonic wave propagation of 150 kHz is cylindrical at near field depth (1.5 cm). The maximum pressure level was observed in the near field depth with 140 kPa acoustic pressure and 0.35 MI at 0.20 W/cm<sup>2</sup> intensity and 150 kHz frequency. The MI at a near distance of the transducer was 0.26 while it is 0.01 at a distance of 3 cm. The near field depth of 40 kHz frequency is 0.4 cm from the transducer. 100 kPa acoustic pressure at near field depth was observed for 40 kHz frequency and 0.23 W/cm<sup>2</sup> intensity with 0.50 MI value. However, the highest MI was estimated to be 0.70 at 0.1 cm from the ultrasonic transducer. The lowest MI was 0.13 cm at 3 cm, which was achieved by propagating acoustic pressure in the water environment. The 28 kHz ultrasonic transducer with 0.30 cm near field depth shows more divergence. The acoustics pressure average at 0.30 cm distance was estimated to be 27.3 kPa. In near field depth of 28 kHz frequency and 0.02 W/cm<sup>2</sup> intensity, acoustics pressure is maximum. The mechanical index values are the highest (0.20) in the near field depth.

The MI is influenced by the intensity and the frequency. The frequency reduction leads to an increase in MI. An increase in the intensity of low-frequencies results in elevating the number of MI. 40 kHz frequency was selected at 0.12-0.35 W/cm<sup>2</sup> intensity at the target surface with a 1.8 cm radius. In this study, the acoustic cavitation interactions were estimated by the MI threshold between 0.10 to 0.80 (3.0 cm to 0.1 cm) from the 40 kHz transducer, selected because of the access to different practical intensities from 0.12 to 0.35 W/cm<sup>2</sup> (<0.50 W/cm<sup>2</sup>), and having the MI threshold of 0.20, more (0.4) or less (0.1).

In 0.20 (threshold MI), more or less than it, axis curves of 40 kHz are plotted along the radial axis of the transducer (Figure 2d-f). The selected radius is the target radius (i.e., culture plate). Maximum MI (40 kHz) for 0.12 (3 cm), 0.23 (2.5 cm), and 0.30 (1 cm) W/cm<sup>2</sup> intensities were calculated to be 0.10, 0.20, and 0.40,

respectively (Figure 2d-f).

Various distances were selected to investigate the MI (threshold, higher and lower) at low intensities of 40 kHz frequency. With 0.12 W/cm<sup>2</sup> intensity (a 3-cm distance from the transducer surface), 0.23 W/cm<sup>2</sup> intensity (a 2.5-cm distance from the surface transducer), and 0.30 W/cm<sup>2</sup> intensity (1.0 cm distance from the surface transducer), the maximum mechanical indices are 0.10 (Figure 2d), 0.20 (Figure 2e), and 0.4 (Figure 2f), respectively. In Figure 2d, the color changes from blue to red, indicating that MI increased from 0.09 to 0.12 by the minimum acoustic pressure of 19 to 24 kPa. Figure 2e shows the MI changes from 0.14 to 0.20 with the minimum pressure changes from 28 to 39 kPa. Figure 2f illustrates the minimum pressure changes from 38 to 86 kPa with the MI range of 0.19 to 0.43. Indeed, the MI is dependent on the intensity of ultrasound waves, leading to increasing MI with increasing intensity. A 40 kHz frequency was selected due to the access to the threshold of the MI range. The treatment groups evaluated consisted of 0.10, 0.20, and 0.40 MI, with different intensities of 0.12, 0.23, and 0.30 W/cm<sup>2</sup> in 3, 2.5, and 1 cm from the transducer and also control and sham groups in a continuous mode and pulse mode.

To reduce the thermal effects of ultrasound waves (<1 °C), sonication time at 0.12 W/cm<sup>2</sup> (MI=0.10) was about 224 s; at 0.23 W/cm<sup>2</sup> (MI=0.20), it was about 140 s; and at 0.30 W/cm<sup>2</sup> (MI=0.40), it was about 105 s with continuous mode. Also, sonication times were about 730, 256, and 226 s at MI values of 0.10, 0.20, and 0.40 with pulse mode, respectively. The repeatability error is less than 1%. The exposure time was obtained from the results of thermal control by a micro thermocouple at continuous and pulse modes. The time needed for a 1 °C rise in temperature was selected as the exposure time of low-frequency LIUS in MI groups.

The sonication was applied to fibroblast cells 24 h after cells adhered to the culture plate.

Table 1 presents the sonication conditions (intensity, distance, sonication time) for each MI.

At about 9-10 days after the tissue explants adhered to the plats, fibroblast cells were observed surrounding the edge of these tissue pieces (Figure 3a). The cells indicated normal fusiform morphology with centrally located oval nuclei (Figure 3b and c). The morphology of fibroblast cells was shown for 0.20 and 0.40 MI groups under continuous mode sonication (Figure 3d-f) and 0.40 MI group under pulse mode sonication (20%)

(Figure 3g) compared to the control group (Figure 3e). These groups are significantly different from the control groups. The morphology of fibroblast cells was shown for 0.20 and 0.40 MI groups under sonication with continuous mode (Figure 3a-b) and 0.40 MI group under sonication with pulse mode (20%) (Figure 3f) compared to the control group (Figure 3g). These are significantly different from the control groups.

The effect of low-frequency LIUS on 10,000 fibroblast cells was investigated in 10% FBS

**Table 1:** The sonication conditions of 40 kHz for each mechanical index (MI).

MI	Intensity (W/cm <sup>2</sup> )	Distance (cm)	Sonication time continuous mode (s)	Sonication time 20% pulse mode (s)
0.10	0.12	3.0	224	730
0.20	0.23	2.5	140	256
0.40	0.30	1.0	105	226

MI: Mechanical Index

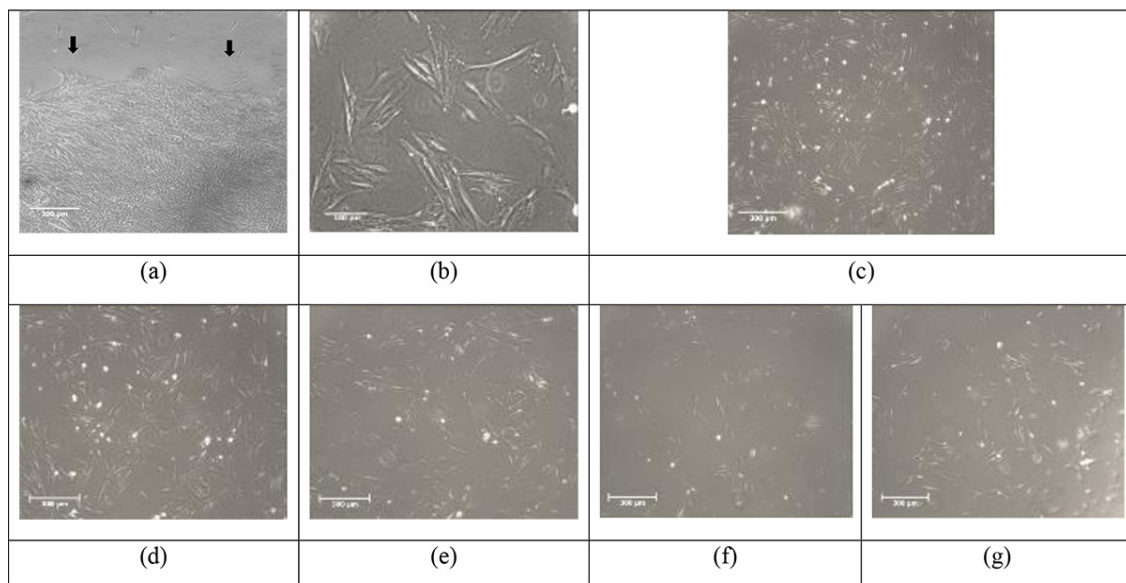


**Figure 3:** Characterization of guinea pig fibroblast cells: **a)** fibroblast cells surrounding explant tissue ( $\times 40$ ), **b)** adherent and fibroblast morphology ( $\times 100$ ), **c)** demonstrating a more spindle-shaped morphology at a confluence of  $>80\%$  ( $\times 40$ ). The morphology of fibroblast cells ( $\times 40$ ) in groups of; **d)** 0.20 MI (Mechanical Index) with continuous mode, **e)** 0.40 MI with continuous mode, **f)** 0.40 MI with pulse mode (20%), and, **g)** control.



culture medium under ultrasonic transducer radiation of 40 kHz with 0.10, 0.20, and 0.40 mechanical indices, 0.12, 0.23, and 0.30 W/cm<sup>2</sup> intensities, and 224, 140, and 105 s exposure time in continuous mode, and 730, 256, and 226 s in 20% pulse mode for 3 consecutive days. Treatment groups were compared with sham and control groups. The cell proliferation was evaluated using the MTT assay after five days (Figure 4a-c). The proliferation index was calculated based on 570 nm optical density on the 5<sup>th</sup> day relative to an optical density at zero-day by the standard curve of fibroblast cells.

According to Figure 4a, there is no significant difference between the sham and control

groups ( $P$ -value>0.05,  $P$ -value=0.798). Increasing reproducibility showed that 0.2 MI group with the  $1.70\pm0.05$  times and 0.40 MI with the  $1.40\pm0.03$  times had the maximum reproducible, and 0.10 MI with  $1.05\pm0.05$  times had the least reproducibility compared to the control group at continuous mode (Figure 4a). There is a significant difference between 0.20 and 0.40 MI groups with other groups ( $P$ -value<0.05). Increasing reproducibility was observed in groups 0.10 and 0.20 MI and with pulse mode of  $1.04\pm0.01$  times and  $1.07\pm0.04$  times compared to the control. Also, a significant difference is between the 0.20 MI group with other groups ( $P$ -value<0.05). Reducing the proliferation in group 0.40 MI was noticed

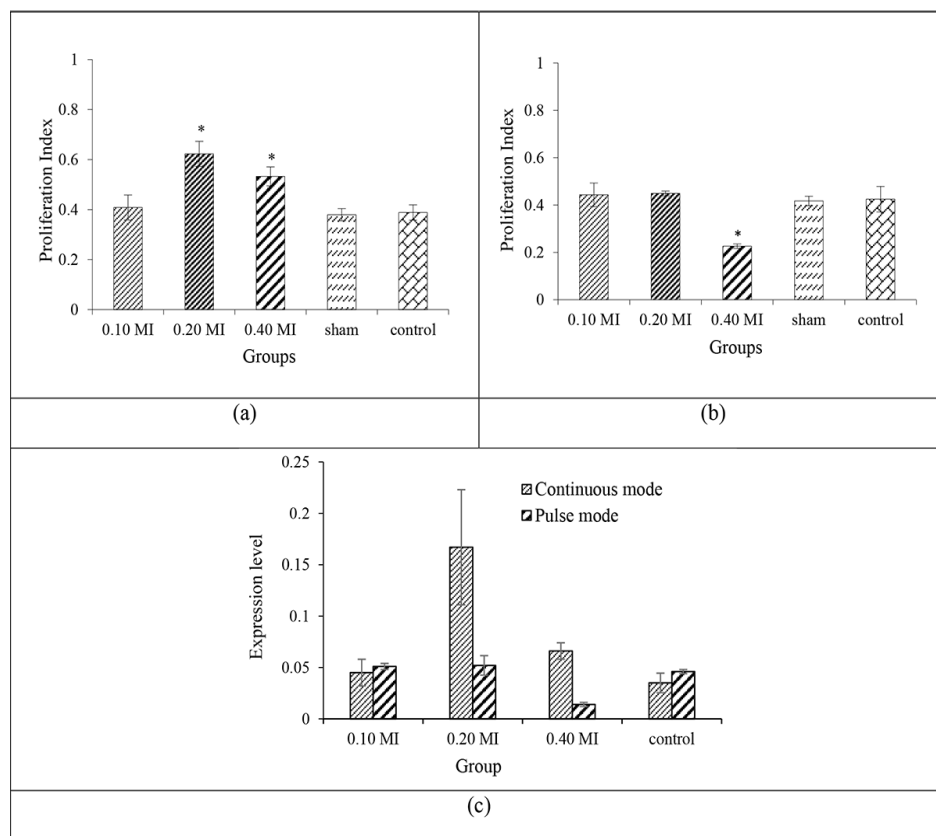


**Figure 4:** Comparison of the proliferation index of cultured cells after 5 days in control, sham, and MI (Mechanical Index) groups with 0.12, 0.20, and 0.30 W/cm<sup>2</sup> intensity: **a)** continuous mode, and **b)** pulse mode. **c)** the effect of MI on collagen type I expression of fibroblast cells with continuous mode and pulse mode (20%) sonication. Markers (\*) represented the significance level.

compared to the control and sham groups at pulse mode ( $P$ -value $<0.05$ ). The results illustrated that the effects of low-frequency LIUS on cell proliferation are parameter-dependent and LIUS with 0.20 MI has the highest impact on proliferation in continuous mode.

Obtained fibroblast cells have a spindle-shaped morphology (Figure 3). Increasing proliferation was shown in the 0.20 MI group under continuous mode sonication with 40000 cells after 5 days. The morphological images confirmed the proliferation index. The effect of MI on the expression level of the collagen I gene was compared with the control group using real-time PCR analysis (Figure 4c). The expression level of collagen type I on fibroblast cells in 0.23 W/cm<sup>2</sup> at the threshold of acoustic cavitation with 0.20 MI was achieved to be  $0.17 \pm 0.05$  compared to the control group, which was  $0.03 \pm 0.00$ . Accordingly, it is seen that collagen I fibroblast cells has increased ( $P$ -value $<0.05$ ). Fold change in the expression level of fibroblast cells in 0.20 MI was achieved 4.35 times compared to the control group. The results show that there is a significant correlation between cell proliferation and collagen I expression level at continuous and pulse modes ( $R=0.91$ ,  $P$ -value $<0.05$ ).

## Discussion

The bio-stimulated effects of low-frequency and also low-intensity ultrasound waves on cell proliferation are influenced by the frequency, intensity, distance, time, and radiation mode. Accordingly, it is necessary to extract optimal treatment parameters. Regarding the importance of the effect of mechanical stimulus on cells, the present study demonstrates that fibroblast cells can be stimulated by 0.2 mechanical index under specific treatment conditions (i.e., radiation mode, intensity, and distance). The benefits of this type of stimuli are safe, non-invasive, non-ionization, and easy to handle.

Low-frequency and low-intensity ultrasound waves are propagating pressure waves that

can transfer mechanical energy into the tissues and cells with applications, such as tissue regeneration stimulus and protein synthesis in fibroblasts and wound healing. Ultrasound therapy has a purely non-thermal function and can trigger intracellular signal transduction and subsequent gene transcription through mechanical interactions on the cellular membrane and cytoskeletal structures [4]. As low-frequency ultrasound waves come through the cell, the mechanical interactions of ultrasound stimulate integrins and receptors on membrane cells. FAK (Focal Adhesion Kinase) and Src (Steroid Co-activator) are intracellular (non-receptor) tyrosine kinases that play important functions in integrin-mediated signal transductions that contribute to promoting a wide range of cellular responses [11, 12].

Acoustic cavitation can be produced as stable states (i.e., radiation force, micro-streaming, and expansion) and inertial states (i.e., shock wave, jet formation, and collapse). At a stable state, the bubbles vibrate around the equilibrium radius and transmit into the cell via an integrin acting as a mechanoreceptor, promoting the attachment of various focal adhesion adaptor proteins to increase proliferation and gene expression [24]. However, in transient cavitation, the bubbles grow rapidly and expand and collapse sharply during a single acoustic compression cycle. Acoustic cavitation interaction could be lethal to cells [25, 26]. Ter Haar's study showed that low-intensity ultrasound may alter cell structure and functioning, attributed to its transient acoustic cavitation effect as well as a change in volume and pressure caused by acoustic cavitation formed in the liquid medium. A change in the pressure exerted by acoustic cavitation may modify the permeability of the cellular membrane to calcium and sodium ions, increasing protein synthesis in cells [1].

Tissues and cell lines derived from animal models are ideal sources to study mechanical stimuli on proliferation and gene expression. Fibroblasts as a form of cell in the

connective tissue are critical to the restoration and remodeling of tissue after injury [5]. The techniques currently utilized to obtain fibroblasts from skin tissues include explant (the growth of cells from cultured tissues) and mechanical or enzymatic degradation methods. In this study, fibroblast cells were obtained by explant outgrowth of guinea pig skin. In Figure 3a, fibroblast-like cells migrate from the skin explants after 9-10 days. The hair patterns and skin characteristics of the guinea pig are more human-like than other rodents [27]. According to this method, the primary passages of these fibroblasts can also be used to evaluate gene expression and proliferation. The advantage of this protocol over enzymatic methods includes achieving more cells in any small amount of skin tissue, a simple, convenient, and rapid procedure.

MI values obtained in 40 kHz with various intensities are more than other frequencies. It has been shown that 40 kHz frequency has positive effects on chronic wound healing rates, proliferation, and migration of cells [28]. Ebrahimi et al. [29] explored the parameters of exposure in low-intensity in near fields of 40 kHz by iodide chemical dosimeter in pulse and continuous modes. He showed the dosimeter absorbance in continuous mode was more than in pulse mode. These results are consistent with the results of the present study (Figure 2).

In this study, the acoustic cavitation threshold (0.20) for stable cavitation (a low-frequency at a 0.23 W/cm<sup>2</sup> intensity, 140 s for 3 consecutive days) showed a significant increase in the cell proliferation. Doan et al. [30] compared 1 MHz frequency, 20% pulsed mode, at 0.1, 0.4, 0.7, and 1.0 W/cm<sup>2</sup> with 45 kHz frequency at 5, 15, 30, and 50 mW/cm<sup>2</sup> at a continuous mode. The best effects on cell proliferation and collagen/non-collagenous protein synthesis are achieved by a 45 kHz continuous mode sonication. Yoon et al. [31] showed 40 kHz frequency and 25 to 35 mW/cm<sup>2</sup> intensity increases mesenchymal stem cell proliferation

derived from a human umbilical cord.

Also, group 0.30 W/cm<sup>2</sup> with 0.40 MI indicated a decrease in the optical density ( $0.22 \pm 0.00$ ) compared to the control group  $0.41 \pm 0.01$  and sham  $0.42 \pm 0.05$  in the pulsed mode. These results show the difference in the effect of the possible interaction of continuous and pulse modes in the culture medium at 40 kHz frequency. An MI higher than 0.20 has a harmful effect on the fibroblast cells in pulse mode because microbubbles rupture at a higher MI and higher intensity leads to activation of the signal pathway for cell death. Thus, incorporating the cavitation threshold of different materials is necessary to find effective parameters for proliferation for the applied frequencies. Oliveira et al. (2011) [32] studied the effects of LIUS with 0.20 and 0.60 W/cm<sup>2</sup> on fibroblast cell cultures. According to the results, intensity is important as an initial parameter for the optimal use of therapeutic ultrasound waves. Furthermore, low intensities decrease cell damage and induce the proliferation of fibroblast cells.

Sonication mode is important because the continuous mode presented significantly higher proliferation effects than the pulsed mode at 40 kHz frequency. Man et al. (2012) [33] investigated the effects of continuous 45 kHz (25 mW/cm<sup>2</sup>) and pulsed 1 MHz (250 mW/cm<sup>2</sup>) ultrasound waves for 30 min (2 days) on osteoblast cells. Continuous kHz ultrasound waves mainly promoted in vitro wound closure by enhancing osteoblast proliferation and cellular migration. The results showed the effect of LIUS with low frequencies, continuous mode, and constant temperature on the cell proliferation.

Low-frequency LIUS applies mechanical interactions. Then, intracellular signaling pathways for transcription of the collagen type I gene are activated. The mechanical stimulation of type I collagen primer (alpha 1 type I collagen) was recorded in the gene bank for a Hartly Dunkin guinea pig specimen and published on the NCBI site to investigate

the collagen expression of fibroblast cells. The expression level of collagen type I in  $0.23 \text{ W/cm}^2$  with  $0.17 \pm 0.05 \text{ MI}$  was compared to that of the control group ( $0.03 \pm 0.00 \text{ MI}$ ). With  $0.17 \text{ MI}$ , collagen type I in fibroblast cells increased significantly. Tang et al. [8] showed in the fibroblast growth factor with low-intensity sonication, the expression of collagen I and collagen II was increased. In these types of studies, the MI of the ultrasound waves was not mentioned. In Tang's study, the distance to the transducer was not set, and only intensity was selected for experimental testing. Tassinari et al. [5] immersed cells in water and sonicated them for the creation of sterile conditions and setting a medium temperature. In the present study, sonication was performed under sterile conditions and in a  $37^\circ\text{C}$  incubator. The sonication time was determined based on the medium temperature.

In the current study, LIUS with  $0.20 \text{ MI}$  at  $0.23 \text{ W/cm}^2$  (continuous wave) significantly increased the proliferation rate and collagen type I expression. Therefore, according to the mechanical index modeling, low-intensity ultrasound waves at the mechanical index threshold, and stable cavitation, dermal fibroblasts enhance through intracellular signal pathways, such as the MAPK pathways (integrin/Mitogen-activated Protein Kinase). Therefore, the cavitation threshold of different materials, environments, and cells is needed to determine their effects.

## Conclusion

It is concluded that fibroblast cell proliferation and collagen type I expression increase on the mechanical index threshold (cavitation threshold) at the continuous mode of  $40 \text{ kHz}$  frequency and,  $0.23 \text{ W/cm}^2$  intensity.

## Acknowledgment

This study was approved by the Faculty of Medical Sciences, Tarbiat Modares University. This study was supported in part by the Iran National Science Foundation (INSF).

## Authors' Contribution

Z. Hormozi Moghaddam, M. Mokhtari-Dizaji, MA. Nilforoshzadeh, and M. Bakhshandeh made substantial contributions to the text and approved the definitive proof. This research work was proofread and supervised by M. Mokhtari-Dizaji and other authors. All the authors read, modified, and approved the final version of the manuscript.

## Ethical Approval

The study was approved by the Ethics Committee Faculty of Medical Sciences, Tarbiat Modares University (Ethics code: IR.TMU.REC.1395.541).

## Conflict of Interest

None

## References

1. Ter Haar G. Therapeutic applications of ultrasound. *Prog Biophys Mol Biol.* 2007;**93**(1-3):111-29. doi: 10.1016/j.pbiomolbio.2006.07.005. PubMed PMID: 16930682.
2. Paliwal S, Mitragotri S. Therapeutic opportunities in biological responses of ultrasound. *Ultrasonics.* 2008;**48**(4):271-8. doi: 10.1016/j.ultras.2008.02.002. PubMed PMID: 18406440.
3. Lv Y, Nan P, Chen G, Sha Y, Xia B, Yang L. In vivo repair of rat transected sciatic nerve by low-intensity pulsed ultrasound and induced pluripotent stem cells-derived neural crest stem cells. *Bio-technol Lett.* 2015;**37**(12):2497-506. doi: 10.1007/s10529-015-1939-5. PubMed PMID: 26303432.
4. Claes L, Willie B. The enhancement of bone regeneration by ultrasound. *Prog Biophys Mol Biol.* 2007;**93**(1-3):384-98. doi: 10.1016/j.pbiomolbio.2006.07.021. PubMed PMID: 16934857.
5. Tassinari JAF, Lunardelli A, Basso BS, Dias HB, Catarina AV, Stülp S, et al. Low-intensity pulsed ultrasound (LIPUS) stimulates mineralization of MC3T3-E1 cells through calcium and phosphate uptake. *Ultrasonics.* 2018;**84**:290-95. doi: 10.1016/j.ultras.2017.11.011. PubMed PMID: 29182945.
6. Karsdal MA. Biochemistry of collagens, Laminins and elastin. 2nd ed, Academic Press; 2019. p. 56-67.
7. Wang KH, Chan WP, Chiu LH, Tsai YH, Fang CL, Yang CB, et al. Histological and Immunohisto-



- chemical Analyses of Repair of the Disc in the Rabbit Temporomandibular Joint Using a Collagen Template. *Materials (Basel)*. 2017;**10**(8):924. doi: 10.3390/ma10080924. PubMed PMID: 28792464. PubMed PMCID: PMC5578290.
8. Tang ZF, Li HY. Effects of fibroblast growth factors 2 and low intensity pulsed ultrasound on the repair of knee articular cartilage in rabbits. *Eur Rev Med Pharmacol Sci*. 2018;**22**(8):2447-53. doi: 10.26355/eurrev\_201804\_14838. PubMed PMID: 29762847.
9. Harding KG, Morris HL, Patel GK. Science, medicine and the future: healing chronic wounds. *BMJ*. 2002;**324**(7330):160-3. doi: 10.1136/bmj.324.7330.160. PubMed PMID: 11799036. PubMed PMCID: PMC1122073.
10. Sorrell JM, Caplan AI. Fibroblast heterogeneity: more than skin deep. *J Cell Sci*. 2004;**117**(Pt 5):667-75. doi: 10.1242/jcs.01005. PubMed PMID: 14754903.
11. Sato M, Nagata K, Kuroda S, Horiuchi S, Nakamura T, Karima M, et al. Low-intensity pulsed ultrasound activates integrin-mediated mechanotransduction pathway in synovial cells. *Ann Biomed Eng*. 2014;**42**(10):2156-63. doi: 10.1007/s10439-014-1081-x. PubMed PMID: 25096496.
12. Takeuchi R, Ryo A, Komitsu N, Mikuni-Takagaki Y, Fukui A, Takagi Y, et al. Low-intensity pulsed ultrasound activates the phosphatidylinositol 3 kinase/Akt pathway and stimulates the growth of chondrocytes in three-dimensional cultures: a basic science study. *Arthritis Res Ther*. 2008;**10**(4):R77. doi: 10.1186/ar2451. PubMed PMID: 18616830. PubMed PMCID: PMC2575623.
13. Tran TA, Roger S, Le Guennec JY, Tranquart F, Bouakaz A. Effect of ultrasound-activated microbubbles on the cell electrophysiological properties. *Ultrasound Med Biol*. 2007;**33**(1):158-63. doi: 10.1016/j.ultrasmedbio.2006.07.029. PubMed PMID: 17189059.
14. Safari M, Ghanati F, Hajnoruzi A, Rezaei A, Abdolmaleki P, Mokhtari-Dizaji M. Maintenance of membrane integrity and increase of taxanes production in hazel (*Corylus avellana* L.) cells induced by low-intensity ultrasound. *Biotechnol Lett*. 2012;**34**(6):1137-41. doi: 10.1007/s10529-012-0865-z. PubMed PMID: 22315099.
15. Hormozi-Moghaddam Z, Mokhtari-Dizaji M, Nilforoshzadeh MA, Bakhshandeh M. Low-intensity ultrasound to induce proliferation and collagen I expression of adipose-derived mesenchymal stem cells and fibroblast cells in co-culture. *Measurement*. 2021;**167**:108280. doi: 10.1016/j.measurement.2020.108280.
16. Zhou S, Schmelz A, Seufferlein T, Li Y, Zhao J, Bachem MG. Molecular mechanisms of low intensity pulsed ultrasound in human skin fibroblasts. *J Biol Chem*. 2004;**279**(52):54463-9. doi: 10.1074/jbc.M404786200. PubMed PMID: 15485877.
17. Moghaddam ZH, Mokhtari-Dizaji M, Movahedin M, Ravari ME. Estimation of the distribution of low-intensity ultrasound mechanical index as a parameter affecting the proliferation of spermatogonia stem cells in vitro. *Ultrason Sonochem*. 2017;**37**:571-81. doi: 10.1016/j.ultsonch.2017.02.013. PubMed PMID: 28427670.
18. Moghaddam ZH, Mokhtari-Dizaji M, Movahedin M. Effect of Acoustic Cavitation on Mouse Spermatogonial Stem Cells: Colonization and Viability. *J Ultrasound Med*. 2021;**40**(5):999-1010. doi: 10.1002/jum.15476. PubMed PMID: 32876351.
19. Church CC, Labuda C, Nightingale K. A theoretical study of inertial cavitation from acoustic radiation force impulse imaging and implications for the mechanical index. *Ultrasound Med Biol*. 2015;**41**(2):472-85. doi: 10.1016/j.ultrasmedbio.2014.09.012. PubMed PMID: 25592457. PubMed PMCID: PMC4297318.
20. Ebrahiminia A, Mokhtari-Dizaji M, Toliyat T. Dual frequency cavitation event sensor with iodide dosimeter. *Ultrason Sonochem*. 2016;**28**:276-82. doi: 10.1016/j.ultsonch.2015.07.005. PubMed PMID: 26384909.
21. Razavi S, Salimi M, Shahbazi-Gahrouei D, Karbasi S, Kermani S. Extremely low-frequency electromagnetic field influences the survival and proliferation effect of human adipose derived stem cells. *Adv Biomed Res*. 2014;**3**:25-31. doi: 10.4103/2277-9175.124668. PubMed PMID: 24592372. PubMed PMCID: PMC3928843.
22. Hashimoto T, Kojima K, Tamada Y. Higher gene expression related to wound healing by fibroblasts on silk fibroin biomaterial than on collagen. *Molecules*. 2020;**25**(8):1939. doi: 10.3390/molecules25081939. PubMed PMID: 32331316. PubMed PMCID: PMC7221890.
23. Hormozi Moghaddam Z, Mokhtari-Dizaji M, Nilforoshzadeh MA, Bakhshandeh M, Ghaffari Khaligh S. Low-intensity ultrasound combined with allogenic adipose-derived mesenchymal stem cells (AdMSCs) in radiation-induced skin injury treatment. *Sci Rep*. 2020;**10**(1):20006. doi: 10.1038/s41598-020-77019-9. PubMed PMID: 33203925. PubMed PMCID: PMC7673019.
24. Widegren U, Wretman C, Lionikas A, Hedin G, Henriksson J. Influence of exercise intensity on

- ERK/MAP kinase signalling in human skeletal muscle. *Pflugers Arch.* 2000;**441**(2-3):317-22. doi: 10.1007/s004240000417. PubMed PMID: 11211119.
25. Dougherty CJ, Kubasiak LA, Prentice H, Andreka P, Bishopric NH, Webster KA. Activation of c-Jun N-terminal kinase promotes survival of cardiac myocytes after oxidative stress. *Biochem J.* 2002;**362**(Pt 3):561-71. doi: 10.1042/0264-6021:3620561. PubMed PMID: 11879182. PubMed PMCID: PMC1222419.
  26. Kyriakis JM, Avruch J. Mammalian mitogen-activated protein kinase signal transduction pathways activated by stress and inflammation. *Physiol Rev.* 2001;**81**(2):807-69. doi: 10.1152/physrev.2001.81.2.807. PubMed PMID: 11274345.
  27. Rodgers KE, Tan A, Kim L, Espinoza T, Meeks C, Johnston W, Maulhardt H, Donald M, Hill C, diZerega GS. Development of a guinea pig cutaneous radiation injury model using low penetrating X-rays. *Int J Radiat Biol.* 2016;**92**(8):434-43. doi: 10.1080/09553002.2016.1186302. PubMed PMID: 27258737.
  28. Conner-Kerr T, Malpass G, Steele A, Howlett A. Effects of 35 kHz, low-frequency ultrasound application in vitro on human fibroblast morphology and migration patterns. *Ostomy Wound Manage.* 2015;**61**(3):34-41. PubMed PMID: 25751849.
  29. Ebrahimi A, Mokhtari-Dizaji M, Toliyat T. Correlation between iodide dosimetry and terephthalic acid dosimetry to evaluate the reactive radical production due to the acoustic cavitation activity. *Ultrason Sonochem.* 2013;**20**(1):366-72. doi: 10.1016/j.ultsonch.2012.05.016. PubMed PMID: 22766173.
  30. Doan N, Reher P, Meghji S, Harris M. In vitro effects of therapeutic ultrasound on cell proliferation, protein synthesis, and cytokine production by human fibroblasts, osteoblasts, and monocytes. *J Oral Maxillofac Surg.* 1999;**57**(4):409-19. doi: 10.1016/s0278-2391(99)90281-1. PubMed PMID: 10199493.
  31. Yoon JH, Roh EY, Shin S, Jung NH, Song EY, Lee DS, et al. Introducing pulsed low-intensity ultrasound to culturing human umbilical cord-derived mesenchymal stem cells. *Biotechnol Lett.* 2009;**31**(3):329-35. doi: 10.1007/s10529-008-9872-5. PubMed PMID: 18985278.
  32. Franco de Oliveira R, Pires Oliveira DA, Soares CP. Effect of low-intensity pulsed ultrasound on I929 fibroblasts. *Arch Med Sci.* 2011;**7**(2):224-9. doi: 10.5114/aoms.2011.22071. PubMed PMID: 22291760. PubMed PMCID: PMC3258710.
  33. Man J, Shelton RM, Cooper PR, Landini G, Scheven BA. Low intensity ultrasound stimulates osteoblast migration at different frequencies. *J Bone Miner Metab.* 2012;**30**(5):602-7. doi: 10.1007/s00774-012-0368-y. PubMed PMID: 22752127.